Turbulence Modeling and Experiments

Aamir Shabbir

1. Motivation and Objective

The best way of verifying turbulence models is to do a direct comparison between the various terms and their models[1,2,3]. The success of this approach depends upon the availability of the data for the exact correlations (both experimental and DNS). The other approach involves numerically solving the differential equations and then comparing the results with the data. The results of such a computation will depend upon the accuracy of all the modeled terms and constants. Because of this it is sometimes difficult to find the cause of a poor performance by a model. However, such a calculation is still meaningful in other ways as it shows how a complete Reynolds stress model performs.

In this study thirteen homogeneous flows are numerically computed using the second order closure models. We concentrate only on those models which use a linear (or quasi-linear) model for the rapid term. This, therefore, includes the Launder ,Reece and Rodi[4] (LRR) model; the isotropization of production [4] (IP) model; and the Speziale, Sarkar and Gatski [5] (SSG) model. The purpose of this study is to find out which of the three models performs better and what are their weaknesses, if any.

The other work reported here deals with the experimental balnces of the second moment equations for a buoyant plume. Despite the tremendous amount of activity toward the second order closure modeling of turbulence, very little experimental information is available about the budgets of the second moment equations. Part of the problem stems from our inability to measure the pressure correlations. However, if everything else appearing in these equations is known from the experiment, pressure correlations can be obtained as the closing terms. This is the closest we can come to in obtaining these terms from experiment, and despite the measurement errors which might be present in such balances, the resulting information will be extremely useful for the turbulence modelers. The purpose of this part of the work reported here was to provide such balances of the Reynolds stress and heat flux equations for the buoyant plume.

2.0.0 Work Accomplished

2.1.0 Comparison of Second Order Models in Homogeneous Flows

Before presenting the results a note about the LRR model constants used in the present study is in order. These constants have evolved to slightly different values than those orginally recommended by LRR[4]. The value of the Rotta constant C_1 (in the return to isotropy term) used in the present study is 3.6 (note that due to a different definition of b_{ij} used here the value of C_1 differs by a factor of two). The

rapid term constant C_2' was assigned a value of 0.4 in the original LRR model. In the present study the value used for this constant is 0.55 which is slightly higher than the value of 0.5 recommended by Morris[6]. It was found out that the value of 0.55 led to improvement in the performance of LRR model in all the flows tested here. (The improvements were slight for the irrotationally strained flows but

Figure 1 compares the development of Reynolds stresses computed using these three models in a flow through axisymmetric contraction with the DNS data[7].

Here we show a typical case of $S = 100.00$ ($Sk_o/\epsilon_o = 55.73$, case AXM). All the models deviate from the DNS data. However, LRR model gives slightly better results than the SSG model with IP model performing the worst.

Figures 2 and 3 show a similar comparison for flow through axisymmetric expansion for two different strain rates. For the smaller strain rate flow ($S = 0.717, Sk_o/\epsilon_o =$ .408, case EXO) SSG model reproduces the $\overline{u^2}$development quite well while both IP and LRR models underpredict it. For the $\overline{v^2}$ component all the models give similar results. Therefore, for this low strain rate flow SSG model is better than the other two models. For the flow with higher strain rate ($S = 7.17, Sk_o/\epsilon_o = 4.08$, case EXP) the LRR model is in excellent agreement with the DNS data for both the components while both IP and SSG models show overprediction So for this flow LRR model works the best.

Now we show comparisons for the distortion of turbulence by plane strain for four cases of differing strain rates. We start from the lower strain rate case. Figure 4 compares the evolution of the three non-zero Reynolds stress components for the flow with strain rate $S = 2.6$ ($Sk_o/\epsilon_o = 2.309$, case PXC), For $\overline{u^2}$component all the models underpredict the DNS data. LRR model is slightly better than the SSG model. IP model is the worst of the three. For $\overline{v^2}$ component IP model works the best. LRR model slightly underpredicts $\overline{v^2}$ while SSG overpredicts it. The third component $\overline{w^2}$ is overpredicted by all the models with LRR model being better than the other two. Figure 5 shows the similar comparisons for the highest strain rate case ($S = 25.0, S_ok/\epsilon_o = 22.227$, case PXE). All the three models underpredict the $\overline{u^2}$component. IP model is the worst of the three models. LRR model gives slightly better result than the SSG model for this stress component. For $\overline{v^2}$ component LRR model is the best and SSG model is the worst of the three. For the $\overline{w^2}$ component all the three models overpredict the DNS data with LRR mdoel being closest to the data. From the above four plane strain flow comparisons, we note that the performance of all the three models deteriorates as the strain rate increases. However, on the overall LRR model works better than the other two models.

Figure 6 shows the same comparison with the homogeneous shear flow experiment[8] ($S = 46.8, Sk_o/\epsilon_o = 6.46$). For the $\overline{u^2}$component LRR model gives the best result whereas SSG and IP models overpredict it. For the $\overline{v^2}$ component also the LRR works the best. SSG model slightly overpredicts the data where as IP model if off by a larger margin. For the $\overline{w^2}$ component both SSG and IP models reproduce the data very well whereas LRR model overpredicts the data. For the shear stress component LRR performs reasonably whereas SSG model slightly overpredicts the data and IP model is off the data by a higher margin. So, for this experiment, LRR

model has better overall performance than the other two models.

Last, we discuss the evolution of $\overline{q^2}$ for the case of rotating homogeneous shear flow. Since no experimental or DNS data is available for this flow the comparisons will be made (for two cases) with the LES[9]. Bardina[10] pointed out that in this case we should be careful in interpreting the comparisons for anything more than the trends shown by the LES. In all the cases shown here the initial conditions corresponded to isotropic turbulence with $\epsilon_0/Sk_o = 0.296$. Figure 7 shows the comparisons for the three cases of different Rosby numbers ($= \Omega/S$). For $\Omega/S = .25$ we note that all three models significantly underpredict the LES results for $\overline{q^2}$; SSG being closest to the LES data and the LRR being the furthest. Qualitatively all the three models reproduce the LES trends. For the case of $\Omega/S = 0.50$ SSG is in excellent agreement with the LES results. Both IP and LRR give identical results and give a smaller value of $\overline{q^2}$ than the LES. It should be pointed out that SSG model constants were partially calibrated against this flow. For the third case of $\Omega/S = 1.0$, all the three models give identical results. Since no LES results are available for this case the only purpose of showing the results is to see how the three models compare with each other.

2.1.2 Conclusions

Results were shown from numerical computation of various homogeneous turbulent flows using three different turbulence models. All of these models use a linear (or quasi-linear) model for the rapid part of the pressure strain model. Based on their overall performance it is found that LRR model works better than both SSG and IP models. For the irrotationally flows the differences between the models and DNS data increased with the strain rate with LRR model performing better than the other two models. For the simple homogeneous shear flow LRR model better than the SSG model (for the DNS both performed equally good but for the experiment LRR worked better). For the homogeneous shear flows both SSG and LRR model showed trends similar to those shown by LES with SSG performing better than the LRR model. It is worth noting that SSG model has seven empirical constants as compared to two in LRR model and on the overall it still does not perform better than LRR model. Part of the reason for this may be due to the fact that the SSG model does not satisfy the normalization constraint where as LRR model does. (Normalization is an exact property of the pressure strain correlation; see references 4 and 11 for details.) As has been pointed out by Shih and Lumley[3], for a model of the rapid pressure strain part which is linear in the anisotropic tensor and satisfies all of its *exact* properties, LRR is the most general model.

2.2.0 Experimental Balances for the Second Moments for a Buoyant Plume

2.2.1 Heat Flux Budgets

The transport equation for the vertical (streamwise) heat flux can be written as

$$U\frac{\partial \overline{wt}}{\partial r} + W\frac{\partial \overline{wt}}{\partial z} = -\frac{1}{r}\frac{\partial}{\partial r}(r\overline{uwt}) - \frac{\partial}{\partial z}(\overline{wwt}) - \overline{uw}\frac{\partial T}{\partial r} - \overline{w^2}\frac{\partial T}{\partial z}$$

$$-\overline{ut}\frac{\partial W}{\partial r}-\overline{wt}\frac{\partial W}{\partial z}+g\beta\overline{t^2}-\frac{1}{\rho}\overline{t\frac{\partial p}{\partial z}}-(\nu+\Gamma)\overline{t_{,j}w_{,j}} \qquad (1)$$

Note that the molecular term is written in local cartesian coordinates. The balance of this equation is shown in figure 8. Advection term is the smallest in this balance and, therefore, contributes least to the transport of the heat flux $\overline{wt}$. It is clear that in the central core of the flow ($r/z < 0.04$), the production of this heat flux is maintained by the mean buoyancy gradients and the turbulent buoyancy force i.e. the source of energy is the gravitational field. The shear production is relatively small in this region. Then there is an intermediate region where the production from mean velocity and gravitational field are of the same order. However, for $r/z > 0.1$ (which approximately corresponds to the plume half width), most of the production is maintained by the mean velocity and buoyancy gradients and the turbulent buoyancy production is only a small fraction of these two. The closing term in the heat flux balances is labelled as Π_i and represents the sum of the pressure correlation and the molecular destruction terms i.e.

$$\Pi_i=\frac{1}{\rho}\overline{t\frac{\partial p}{\partial x_i}}-(\nu+\Gamma)\overline{\frac{\partial u_i}{\partial x_j}\frac{\partial t}{\partial x_j}} \qquad (2)$$

The molecular term in (2) is thought to get weaker with increasing Reynolds and Peclet numbers, eventually approaching a value of zero in the limit of local (small scale) isotropy. This term was not measured and, therefore, its magnitude relative to others can not be established. However, in turbulence modeling, it is customary to combine this term with the pressure correlation term[8] and, therefore, from that point of view not knowing each term separately does not reduce the usefulness of these budgets. Notice that the shape of this term is very similar to the shape of the heat flux $\overline{wt}$ and its magnitude remains large throughout the flow field.

The equation for the radial heat flux is

$$\begin{aligned}U\frac{\partial\overline{ut}}{\partial r}+W\frac{\partial\overline{ut}}{\partial z}=&-\frac{1}{r}\frac{\partial}{\partial r}(r\overline{uut})-\frac{\partial}{\partial z}(\overline{wut})-\overline{u^2}\frac{\partial T}{\partial r}-\overline{uw}\frac{\partial T}{\partial z}\\&-\overline{ut}\frac{\partial U}{\partial r}-\overline{wt}\frac{\partial U}{\partial z}-\frac{1}{\rho}\overline{t\frac{\partial p}{\partial r}}-(\nu+\Gamma)\overline{t_{,j}u_{,j}}\end{aligned} \qquad (3)$$

The balance of this equation is shown in figure 9. Again, we note that the advection term is quite small as compared to the other dominant terms in the equation. Unlike the $\overline{wt}$ heat flux balance, the shear production is extremely small here. This is because the gradients of mean radial velocity are much smaller than the gradients in the mean vertical (streamwise) velocity. There is no turbulent buoyancy production in this equation and all the production is due to the mean buoyancy gradients. We note that the term representing sum of the pressure correlation and the molecular destruction makes up a substantial part of the budget and its shape is similar to the radial heat flux. We also note that this budget can not be divided into any subregions, where some phenomenon are more dominant than others, because the relative magnitude of each of the terms in equation (3) remains the same across the flow field.

2.2.2 Reynolds Stress Budgets

The transport equation for the Reynolds stress, within Bussinesq approximation, is

$$U_k\,(\overline{u_iu_j})_{,k} = -\,[\overline{u_iu_ju_k}]_{,k} - (\overline{u_iu_k}\;U_{j,k} + \overline{u_ju_k}\;U_{i,k}) + \beta_i\overline{u_jt} + \beta_j\overline{u_it} + \frac{1}{\rho}(\overline{u_ip_{,j} + u_jp_{,i}}) - 2\nu\overline{u_{i,k}u_{j,k}} \qquad (4)$$

where the viscous diffusion term has been neglected since it will be small as compared to the turbulent diffusion.

For reasons of convenience, turbulence modelers do not model the pressure correlation term in the form as it appears in the above equation but re-write it in a different form by separating it into a deviatoric and a non-deviatoric part. Two ways of doing this have been suggested in the literature and we will look at both of these before deciding which one to use in the present study. The traditional way of writing this term is[4]

$$-\frac{1}{\rho}(\overline{u_ip_{,j} + u_jp_{,i}}) = \frac{1}{\rho}\overline{p(u_{i,j} + u_{j,i})} - \frac{1}{\rho}(\overline{pu_i}\delta_{jk} + \overline{pu_j}\delta_{ik})_{,k} \qquad (5)$$

where the first term on the right hand side is the deviatoric part. The second term is the so called pressure diffusion term. Lumley[12] (1975) has instead suggested the following separation

$$-(\overline{u_ip_{,j} + u_jp_{,i}}) = -\left[\frac{1}{\rho}(\overline{u_ip_{,j} + u_jp_{,i}}) - (\frac{2}{3\rho})(\overline{pu_k})_{,k}\delta_{ij}\right] - (\frac{2}{3\rho})(\overline{pu_k})_{,k}\delta_{ij} \qquad (6)$$

where the term in the square brackets is the deviatoric part and the last term on the right hand side is the pressure diffusion term. Regardless of which separation is employed a correction or model has to be used for the correlation $\overline{pu_k}$. The model used here is due to Lumley[8] is given by $\overline{pu_k} = -\overline{q^2u_k}/5$. This study indicates that the use of this model with (5) produces so much pressure diffusion that it negates the velocity diffusion (i.e. due to $\overline{u_iu_ju_k}$). On this basis it was concluded to use the separation given by (6) in the present study. (For further details see Shabbir[13]).

Therefore, using (6) the equation for the Reynolds stress can be re-written as

$$U_k\,(\overline{u_iu_j})_{,k} = -\left[\overline{u_iu_ju_k} + \frac{2}{3\rho}(\overline{pu_k})\delta_{ij}\right]_{,k} - (\overline{u_iu_k}\;U_{j,k} + \overline{u_ju_k}\;U_{i,k}) - \beta_i\overline{u_jt} - \beta_j\overline{u_it} + \left\{-[\frac{1}{\rho}(\overline{u_ip_{,j} + u_jp_{,i}}) - \frac{2}{3\rho}(\overline{pu_k})_{,k}\delta_{ij}] - 2\nu\overline{u_{i,k}u_{j,k}} + \frac{2}{3}\epsilon\delta_{ij}\right\} - \frac{2}{3}\epsilon\delta_{ij} \qquad (7)$$

where $\epsilon = \epsilon_{ii}$. Note that anisotropic part of the dissipation part has been combined with the pressure correlation term[11]. The term in the curly parenthesis has a zero trace and will be denoted by Φ_{ij} in the rest of the paper. It is this term whose models

have been proposed. Note that the above equation is exact since no approximations have been used so far. Now we introduce the model for the pressure diffusion term, as given above, and with this approximation the above equation becomes

$$U_k\,(\overline{u_iu_j})_{,k} \approx -\left[\overline{u_iu_ju_k} + \frac{2}{15}(\overline{q^2u_k})\delta_{ij}\right]_{,k} - (\overline{u_iu_k}\,U_{j,k} + \overline{u_ju_k}\,U_{i,k}) + \beta_i\overline{u_jt} + \beta_j\overline{u_it} + \Phi_{ij} - \frac{2}{3}\epsilon\delta_{ij} \tag{8}$$

Note that due to the model for the pressure diffusion term this is no longer an exact equation and $\approx$ has been used to emphasize this fact. It is this equation which will be balanced out with the experimental data and the term Φ_{ij} will be obtained as the closing term. It should be reminded that in addition to the measurement errors, any uncertainty in the approximation of the pressure diffusion will also be lumped into Φ_{ij}.

The equation for the streamwise Reynolds stress $\overline{w^2}$ is given by

$$U\frac{\partial\overline{w^2}}{\partial r} + W\frac{\partial\overline{w^2}}{\partial z} \approx -\frac{1}{r}\frac{\partial}{\partial r}(r\overline{uw^2}) - \frac{\partial}{\partial z}(\overline{ww^2}) + \frac{2}{15}\left[\frac{1}{r}\frac{\partial}{\partial r}(r\overline{uq^2}) + \frac{\partial}{\partial z}(\overline{wq^2})\right] - 2\overline{uw}\frac{\partial W}{\partial r} - 2\overline{w^2}\frac{\partial W}{\partial z} + 2g\beta\overline{wt} - \Phi_{zz} - \frac{2}{3}\epsilon \tag{9}$$

The balance of this equation is shown in figure 10. Advection is the smallest of all the terms. Diffusion term is a gain near the center of the plume and a loss in the rest of the flow. Also, its magnitude near the center is comparable to the other dominant terms in the balance. We note that the buoyancy production is comparable to the production due to mean velocity gradients near the plume center but over the rest of the flow field the shear production is much larger than the buoyancy production. It is also interesting to note that the buoyancy production and dissipation rate approximately balance each other. The closing term in this balance is Φ_{zz} and represents the sum of the pressure correlation term and the anisotropic part of the dissipation. This term is a loss for the $\overline{u^2}$ budget and we note that beyond $r/z = 0.08$ this term and shear production approximately balance each other.

The equation for the radial component $\overline{u^2}$ is given by

$$U\frac{\partial\overline{u^2}}{\partial r} + W\frac{\partial\overline{u^2}}{\partial z} \approx -\frac{1}{r}\frac{\partial}{\partial r}(r\overline{uu^2}) - \frac{\partial}{\partial z}(\overline{wu^2}) + \frac{2}{15}\left[\frac{1}{r}\frac{\partial}{\partial r}(r\overline{uq^2}) + \frac{\partial}{\partial z}(\overline{wq^2})\right] - 2\overline{u^2}\frac{\partial U}{\partial r} - 2\overline{uw}\frac{\partial U}{\partial z} - \Phi_{rr} - \frac{2}{3}\epsilon \tag{10}$$

and its balance is shown in figure 11. Obviously the advection of $\overline{u^2}$ has the same form as the advection of $\overline{w^2}$. The production due to velocity gradients is a loss near the plume center and is a gain after about $r/z = 0.04$. This is because the radial gradient of the radial mean velocity is positive near the plume center. The

mechanical production term is not large. The diffusion term is a loss over most of the flow field and becomes a gain toward the outer edge of the flow field. The sum of the pressure correlation term and the anisotropic part of the dissipation rate is obtained as the closing term in the budget and represents a gain for $\overline{u^2}$. We further note that beyond $r/z = 0.08$ it approximately balances the dissipation rate.

Finally we look at the budget for the shear stress $\overline{uw}$ as shown in figure 12. Its equation is given by

$$U\frac{\partial \overline{uw}}{\partial r} + W\frac{\partial \overline{uw}}{\partial z} \approx -\frac{1}{r}\frac{\partial}{\partial r}(r\overline{uuw}) - \frac{\partial}{\partial z}(\overline{wuw}) - \overline{uw}\frac{\partial U}{\partial r} - \overline{uw}\frac{\partial U}{\partial z} - \overline{u^2}\frac{\partial W}{\partial r} - \overline{uw}\frac{\partial W}{\partial z} + g\beta\overline{ut} - \Phi_{rz} \tag{11}$$

Both advection and the turbulent buoyancy production are of very small magnitude and over most of the flow field these approximately balance each other. Neglecting these two terms would not cause any significant change in the shear stress balance. We note that the diffusion term is not negligible in this budget. The term Φ_{rz} is essentially balanced by the difference between the shear production and diffusion processes. The shape of Φ_{rz} is obviously similar to that of the shear stress and its peak approximately corresponds to the peak in the shear production.

3. Future Plans

3.1 Turbulence Modeling (with T.-H. Shih)

(a). Compare the performance of the various non-linear second order models in different homogeneous flows in order to find out their strengths and weakneses. This will be an extension of the work presented in section 1 of this brief.

(b). To develop and test models for turbulent diffusion terms in the Reynolds stress equations using Lumley's theory of third moments[11].

3.2 DNS of Bypass Transistion (with T.-H. Shih and G. Karniadakis).

The bypass transition is an important engineering problem due to its relevence to turbomachinery environment and, therefore, there is a considerable interest both at LeRC and at CMOTT to study this phenomenon. We are interested in carrying out the DNS for this problem both in order to provide a data base for the modeling efforts of bypass transition at CMOTT and to study its physics. For the former we are interesting in finding out what kind of global parameters, if any, are linked to the transition process. For the later we are interested in finding out, for instance, what is the effect of anisotropy in the free stream turbulence velocity and length scale on the transition process.

These simulations will be designed after the experiments of Sohn and Reshotko[14] who studied the bypass transition over a flat plate with differing free stream turbulence intensities. The results of DNS will be compared with these experiments.

3.2.1 Numerical Scheme.

Currently we are exploring the possibility of using a spectral element code for its suitability for doing such a DNS. We are inclined to use a spectral element method because of its higher accuracy and its ease of local grid refinement.

The numerical scheme used in the code involves fractional time discretization which results in three sets of semi discrete equations. In the first step advection term is handled explicitly using a third order Adams-Bashforth scheme. In the second step Poisson equation for pressure is solved implicitly and continuity is satisfied. In the third fractional step the diffusion terms are accounted implicitly by a second order Crank-Nicholson method.

In order to carry out the spatial discretization the flow domain is first decomposed into macro elements. Each of these macro elements uses a local cartesian mesh by employing Gauss-Labatto collocation points. Then within each macro element the flow variables are represented as tensor product of Chebychev polynomial. These representations of the flow variables are then substituted into the governing equations and discrete equations are obtained by applying the weighted residual technique.

3.2.2 Test Cases to be run

Several test cases will have to be run in order to validate the code before a full DNS can be carried out. First of these is to solve the laminar boundary layer flow over a flat plate in order to insure that the numerical method gives the Blasius solution. This will also help us explore the various boundary conditions which can be used at the top boundary and at the outflow and latter can be used for the mean flow during the DNS. After this has been successfully accomplished the most unstable mode disturbances based on the linear stability theory will be intorduced. This will allow comparing their growth rates (in the linear region) with the solutions from the linear stability theory. The third case will be that of suction and blowing through the flat plate and the resutls will be compared with those obtained by previous workers.

4. References

[1] Shabbir, A. and D.B. Taulbee. Evaluation of Turbulence Models for Predicting Buoyant Flows. J. Heat Trans., 112, 945-951 (1990).

[2] Shih, T.-H., A. Shabbir and J.L. Lumley. Advances in the Modeling of Pressure Correlations terms in the Second Moment Equations. NASA TM. 104413 (1991).

[3] Shih,T.-H. and J.L. Lumley. A Critical Comparison of Second Order Closures with Direct Numerical Simulation of Homogeneous Turbulence. NASA TM 105351 (1992).

[4] Launder, B.E., Reece and W. Rodi.Progress in the Development of Reynolds-stress Turbulence Closure. JFM, 68, 537-566 (1975).

[5] Speziale, C.G., S. Sarkar and T.B. Gatski. Modeling the Pressure-Strain Correlation of Turbulence; An Invariant Dynamical Systems Approach. JFM, 227, 245-272, (1991).

[6] Morris, J. Modeling the Pressure Redistribution Terms. Phys. Fluids, 27, 7, 1620-1623 (1984).

[7] Lee, M. and W.C. Reynolds. Numerical Experiments on the Structure of Homogeneous Turbulence. Stanford University Report No. TF-24 (1985).

[8] Tavoularis, S and S. Corrsin. Experiments in Nearly Homogeneous Turbulent Shear Flow with a Uniform Mean Temperature Gradient. Part 1. JFM, 104, 311-347 (1981).

[9] Bardina, J., J.H. Ferziger and W.C. Reynolds Improved Turbulence Models Based on Large-Eddy Simulation of Homogeneous, Incompressible Turbulent Flows. Stanford University Technical Report TF-19 (1983).

[10] Bardina, J. Private communication (1992).

[11] Lumley, J. L. Computational Modeling of Turbulent Flows. Advances in Applied Mechanics, 18, 123-176 (1978).

[12] Lumley, J.L. Phys. Fluids, 18, 750 (1975).

[13] Shabbir, A. of the 8th Symposium on Turbulent Shear Flows (1991).

[14] Sohn, K.-H., and E. Reshotko Experimental Study of Boundary Layer Transition With Elevated Freestream Turbulence on a Heated Flat Plate. NASA CR 187068 (1991).

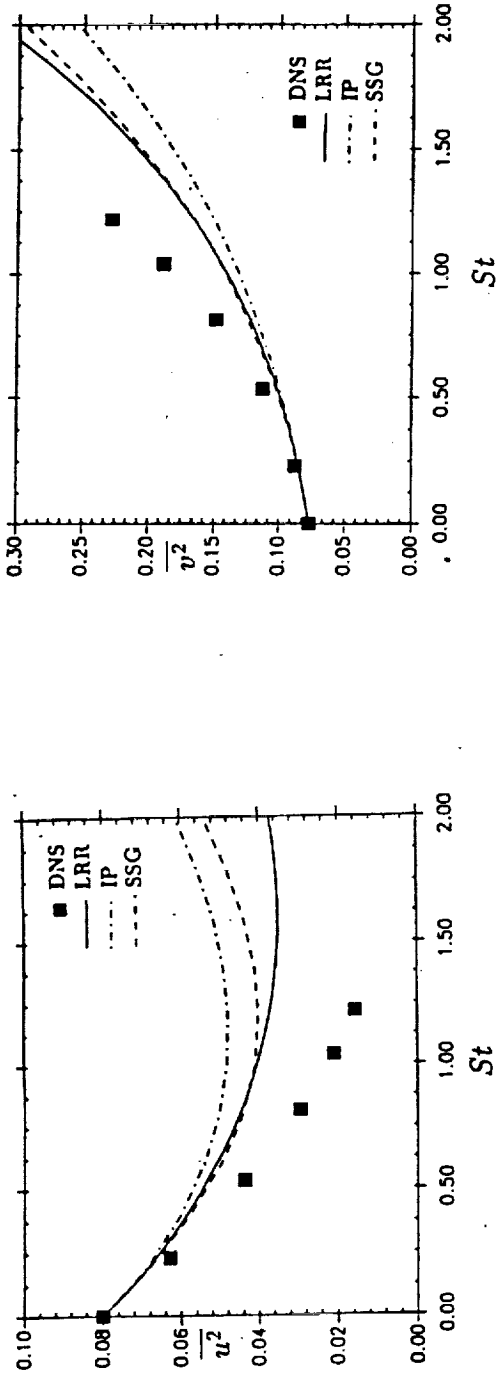

Figure 1. Comparison of the models for flow through axisymmetric contraction with the DNS data of of Lee and Reynolds (1985).

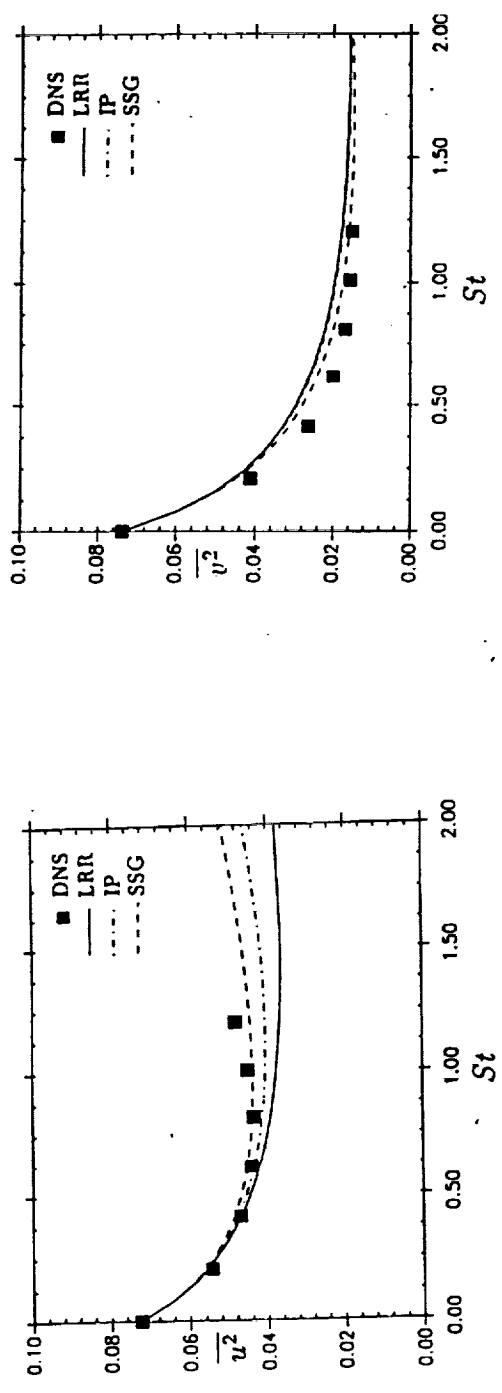

Figure 2. Comparison of the models for flow through axisymmetric expansion with the DNS data of of Lee and Reynolds (1985), case EXO.

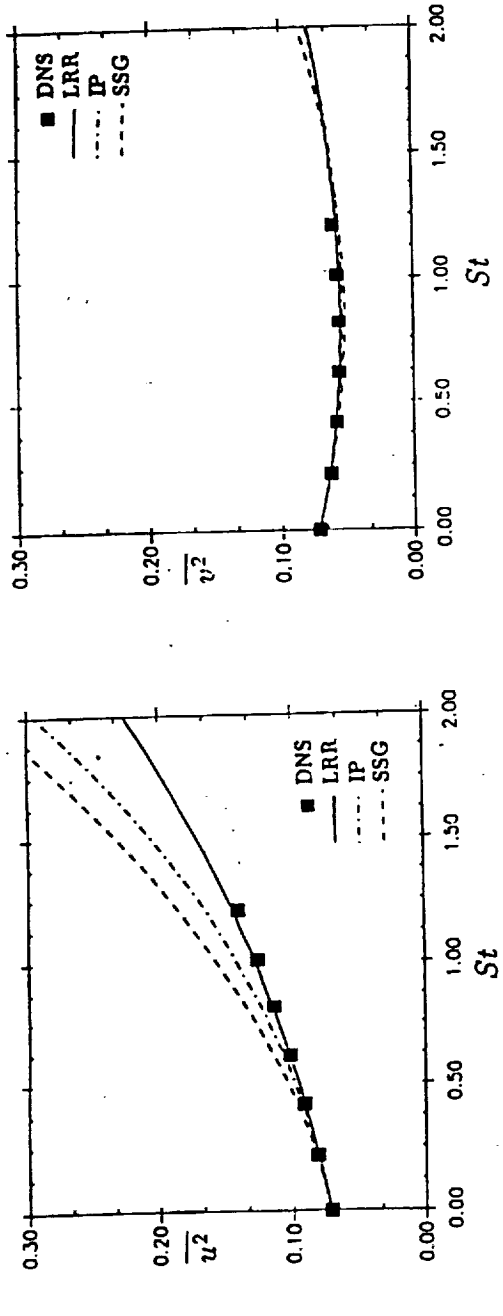

Figure 3. Comparison of the models for flow through axisymmetric expansion with the DNS data of of Lee and Reynolds (1985), case EXP.

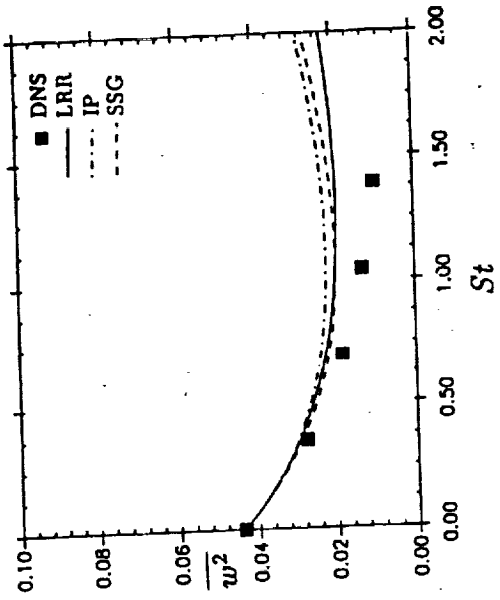

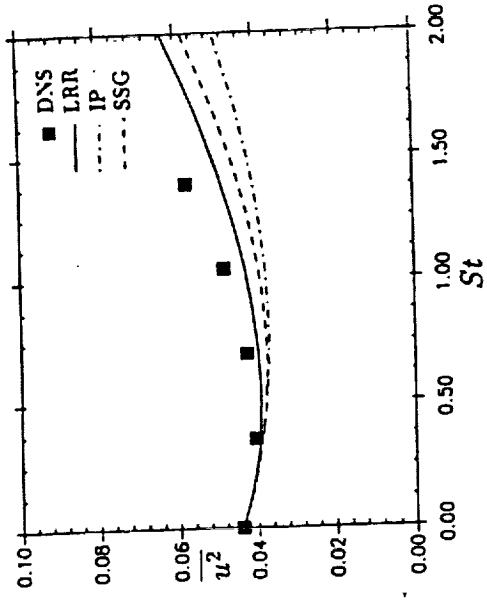

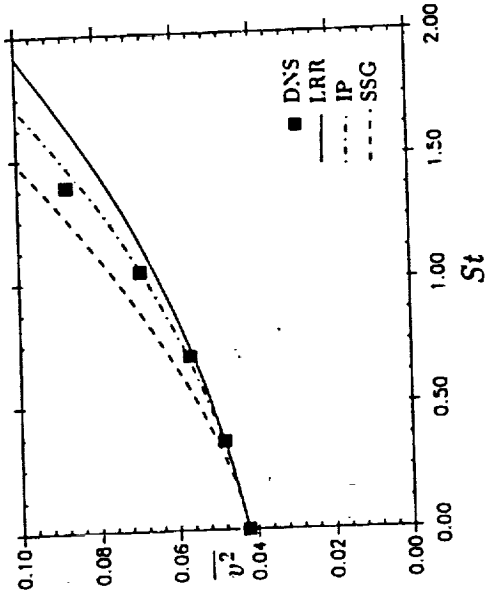

Figure 4. Comparison of the models for distortion by plane strain with the DNS data of Lee and Reynolds (1985), case PXC, S=2.6.

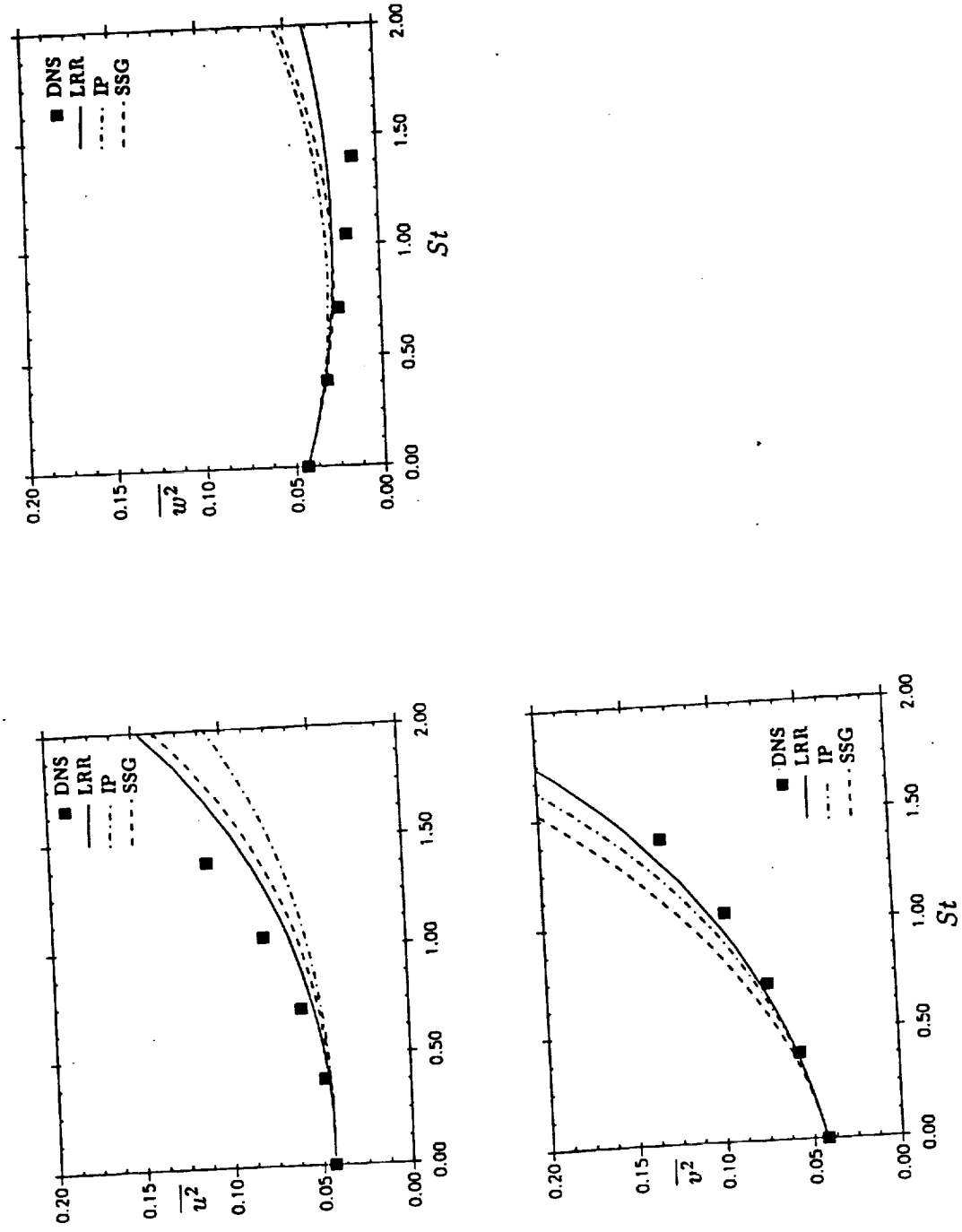

Figure 5 . Comparison of the models for distortion by plane strain with the DNS data of Lee and Reynolds (1985), case PXE, S=25.0

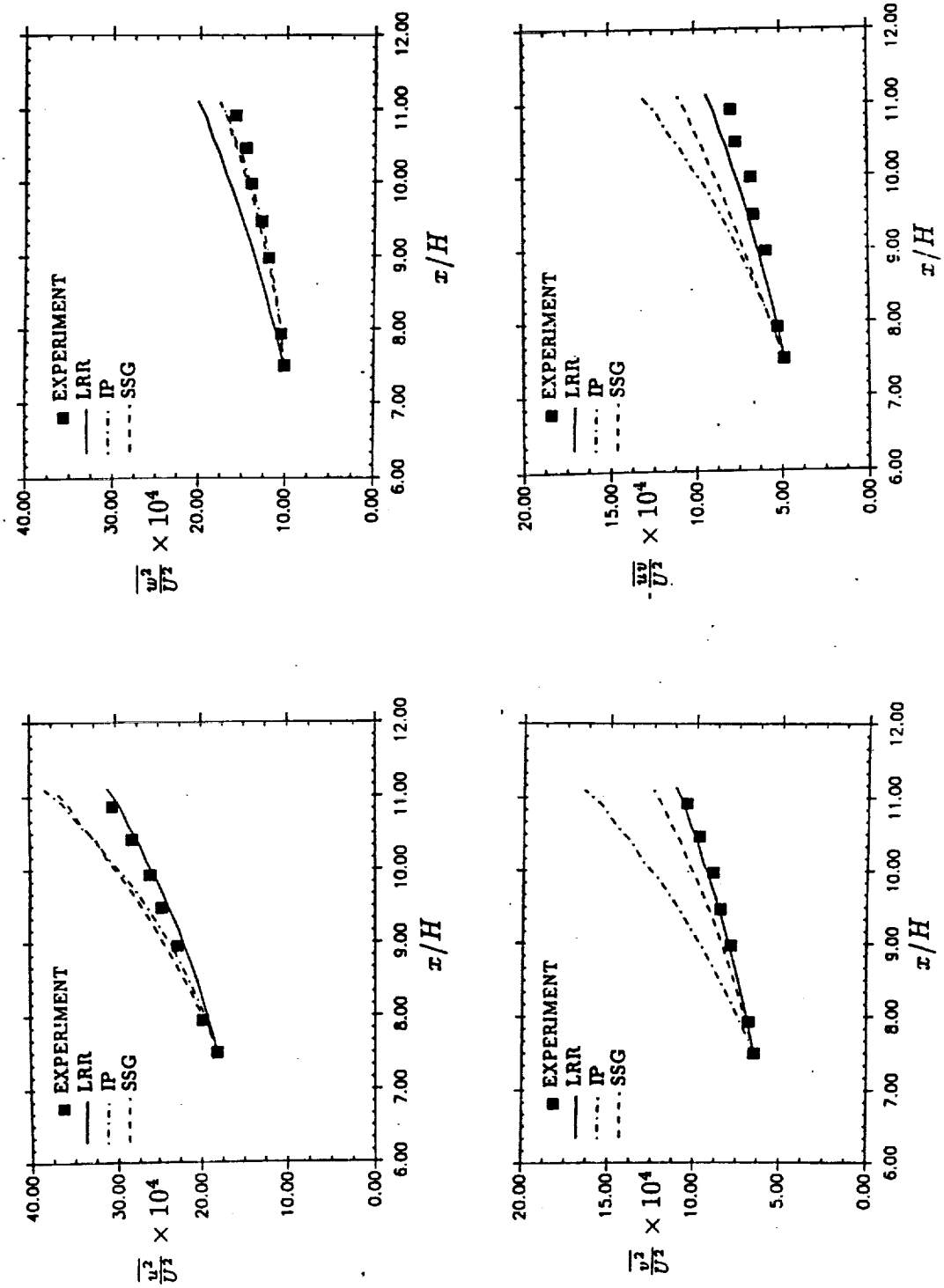

Figure 6 . Comparison of the models for homogeneous shear flow with the data Tavoularis and Corrsin (1981).

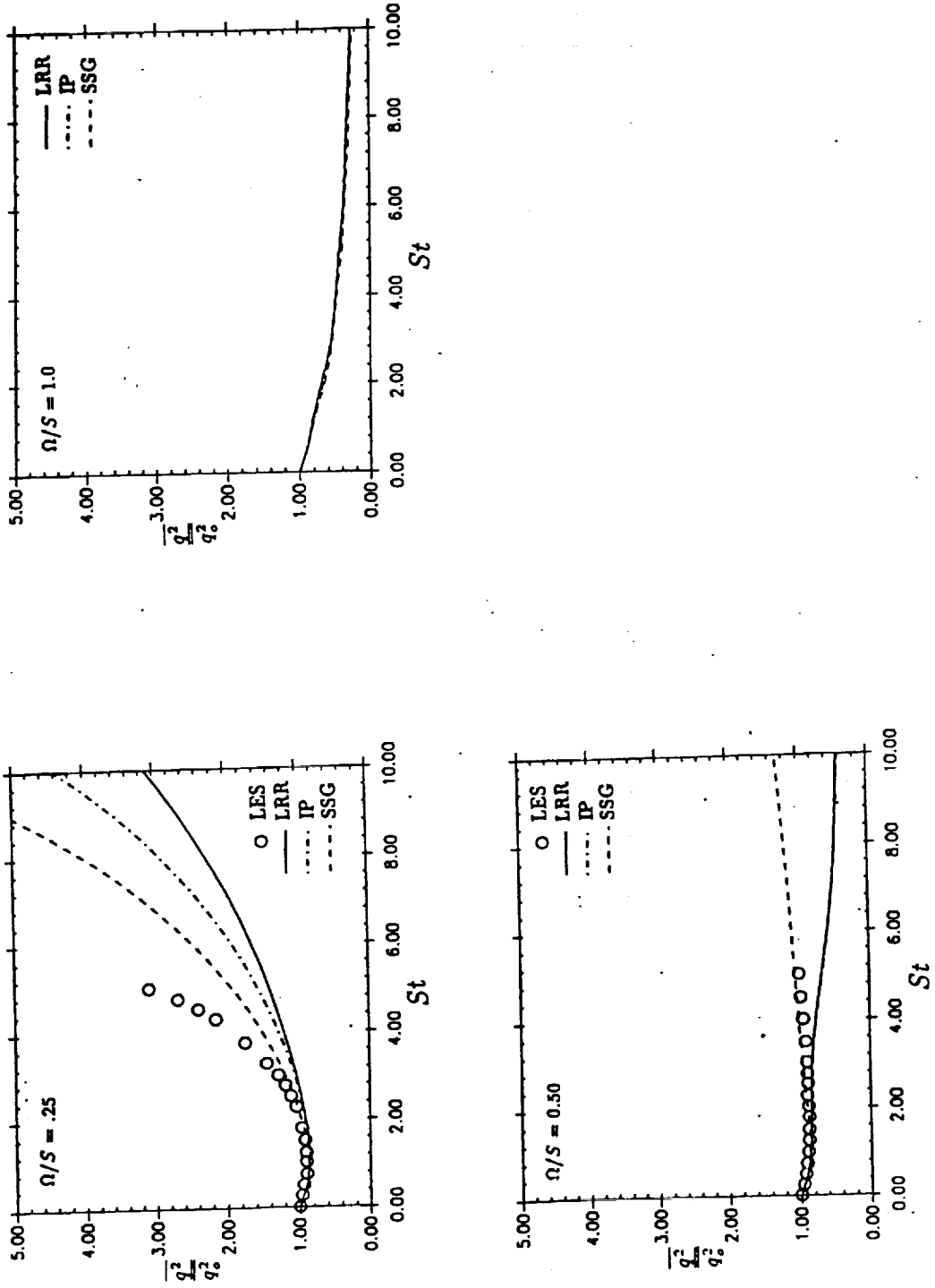

Figure 7.. Comparison of the models for the rotating homogeneous shear flow with the large eddy simulation of Hardina *et al.* (1983).

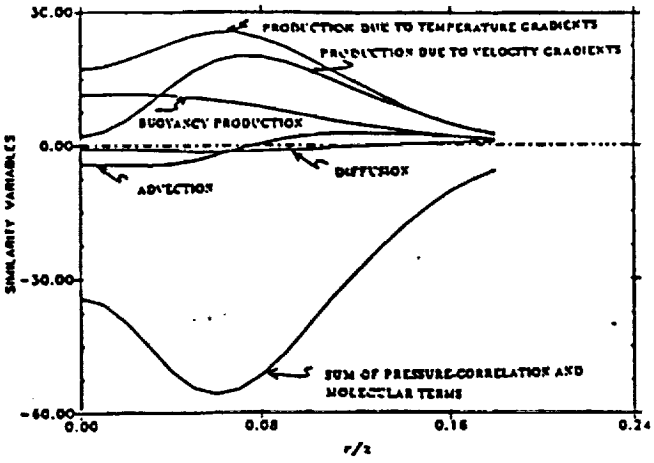

Figure 8 . Budget for $\overline{wt}$ equation.

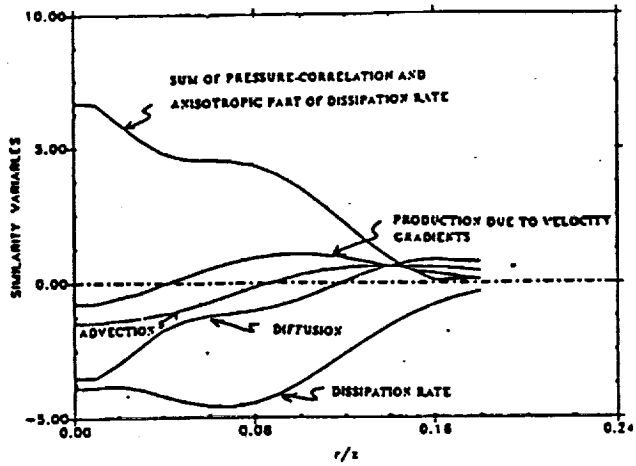

Figure 9 Budget for $\overline{uw}$ equation.

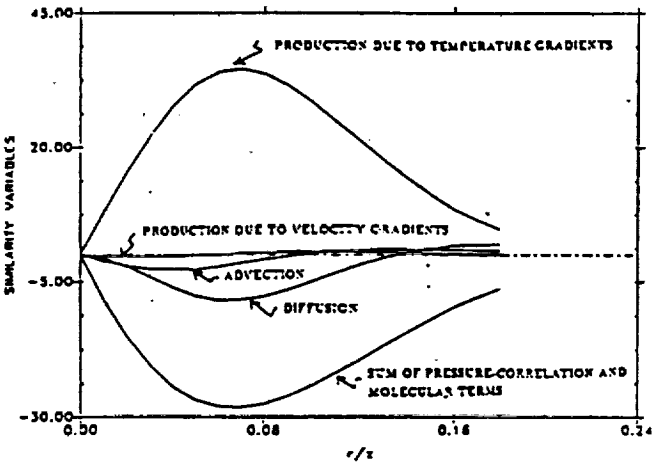

Figure 10. Budget for $\overline{ut}$ equation.

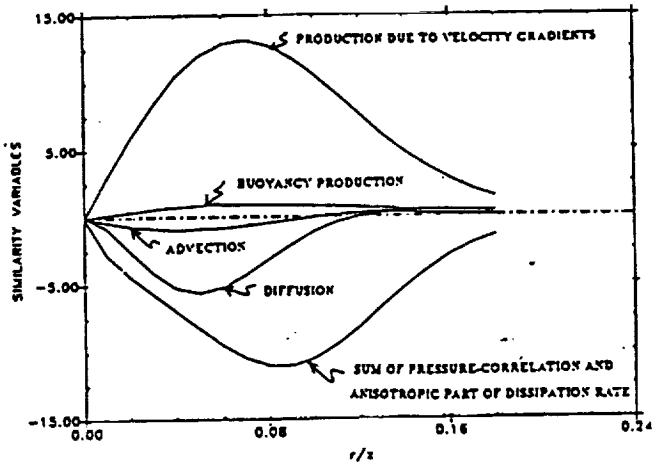

Figure 11. Budget for $\overline{uw}$ equation.

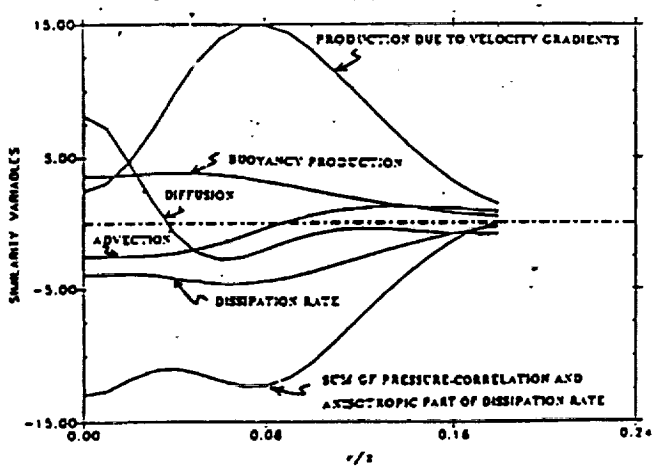

Figure 12. Budget for $\overline{w^2}$ equation.